Chaos in Grinding Process

NICOLAE–DORU STĂNESCU
Department of Applied Mechanics
University of Piteşti
Piteşti, str. Târgul din Vale, 1, jud. Argeş, 110040
ROMANIA
s_doru@yahoo.com

Abstract: - This paper presents a non-linear model for the external grinding of a cylindrical work-piece. A system of non-linear differential equations for the vibrations of the tool and the work-piece is obtained. Non-linearity comes from the cutting force dependence on the feeding velocity and depth of cut. We determine the number of the equilibrium positions, we proved that there exists only one equilibrium position and we study its stability. Results of simulation are discussed. A chaotic regime is found for realistic values of the grinding parameters.

Key-Words: - grinding, equilibrium, stability, chaos

1 Introduction

The accuracy of the ground surfaces is a major concern in grinding processes. The non-uniformity of these surfaces is considered to stem from vibrations arising from the interactions of the tool-work-piece-machine system. This interaction is non-linear due to expressions of the cutting force as a function of the feeding velocity and depth of cut. It is the aim of this paper to investigate the consequences of these non-linearities on the dynamics of the system. In particular we shall examine the possibility of chaotic motions of the tool and work-piece, as might be expected from the nature of the self-excited oscillations the system encounters.

There are two approaches to the understanding of the system dynamics. The direct method consists in modelling this dynamics, whereas the inverse method aims at analysing the experimental time series in order to deduce the nature of the underlying dynamics. Here, we shall model the grinding system, including the work-piece, in order to determine if a chaotic regime can be found. In previous models, only the vibrations of the tool were considered. However, experiments show that the vibrations of the work-piece are of importance for the accuracy of the ground surface. In our model, the tool has two degrees of freedom, while the work-piece has also one degree of freedom, orthogonal to the feeding velocity. The resulting differential equations of motion are coupled through the expression of the cutting force.

2 The Grabec Model

In Grabec model the machine-tool is deformable onto two directions.

Further on, we shall assume that the orthogonal cutting process is described by Fig. 1. The cutting edge of the tool is parallel to the work-piece's surface and normal to the cutting direction.
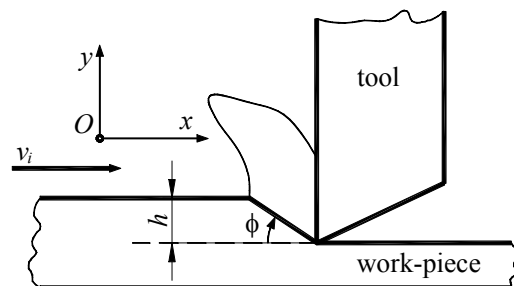

Fig. 1. The Grabec model for the cutting process.

We shall consider that the depth of cut is much smaller than the width of the cutting tool edge, and from this it results a two-dimension model of the cutting process (x, y). In the first direction we assume that there exists a displacement of a homogeneous work-piece by constant speed v_i. Before the cutting process starts the edge of the cutting tool is set to a depth of cut equal to h_i and the cutting edge is $\alpha = 0$.

All the elastic and inertial properties of the machine-tool, of the work-piece and of the tool are represented by a model consisting of two oscillators (Fig. 2). The two oscillators are acted by the cutting force F with its two components F_x and F_y.
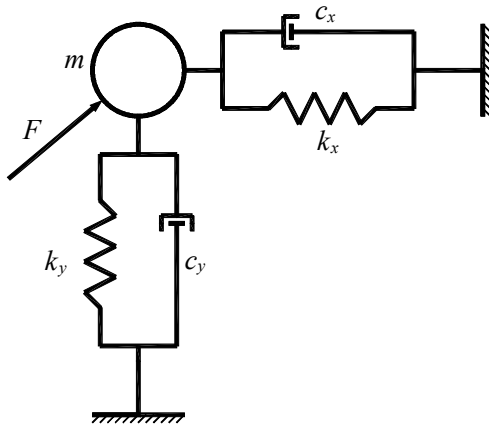
Fig. 2. The mathematical model of the cutting process.

The characteristic variable of the tool's dynamics is its displacement, which can be, decompose onto two reciprocal orthogonal directions. We obtain the equations of motion

$$m\ddot{x} + c_x \dot{x} + k_x x = F_x, \quad m\ddot{y} + c_y \dot{y} + k_y y = F_y. \quad (1)$$

In the previous formulas the mass m is assumed to be the same in both directions. The stiffness and the damping are given by the coefficients k_x, k_y, respectively c_x, c_y.

The cutting force is determined by the geometric, mechanical, and dynamical properties of the work-piece and tool's materials. We shall simplify this diagram reducing it to the dependence of cutting force on the depth of cut h and on the relative speed v between the work-piece and tool and we shall mark this thing by a series of physical constants, which are function of the cutting regime.

The components of the cutting force are depending one on another. If F_x and F_y are considered as the principal cutting force, respectively the friction force, then the interdependence between them can be written with the aid of a friction coefficient K in the form

$$F_y = KF_x. \quad (2)$$

This interdependence makes the two oscillator coupled.

Further on, the properties of the cutting force are described by the dependence of the cutting force and the friction coefficient on the depth of cut and the cutting velocity. For a large class of technical materials the relations between the averaged values can be described by the relations

$$F_x = F_{x_0} \frac{h}{h_0} \left[C_1 \left(\frac{v}{v_0} - 1 \right)^2 + 1 \right], \quad (3)$$

$$K = K_0 \left[C_2 \left(\frac{v}{v_0} - 1 \right)^2 + 1 \right] \left[C_3 \left(\frac{h}{h_0} - 1 \right)^2 + 1 \right]. \quad (4)$$

In these relations the parameters F_{x_0}, K_0, h_0, v_0, C_1, C_2, C_3 are given by the working process's particularities. For simplification, we retained only the quadratic terms.

The friction coefficient is defined by the relative shear speed of the material with respect to the tool into the x direction, but the friction is a consequence of the material's shear along the tool's surface into the y direction. The shear speed v_f into this direction is diminished because of the plastic deformation by a factor R,

$$v_f = \frac{v}{R}. \quad (5)$$

From the dynamical point of view, the friction coefficient is correctly expressed by the following relation

$$K = K_0 \left[C_2 \left(\frac{v_f R}{v_0} - 1 \right)^2 + 1 \right] \times \left[C_3 \left(\frac{h}{h_0} - 1 \right)^2 + 1 \right]. \quad (6)$$

The angle ϕ represents the shear plastic deformation and it is linked to the factor R by the relation

$$R = \cot \phi. \quad (7)$$

The dependence of the share angle on the depth of cut is less significant than the dependence on the cutting speed; therefore the factor R can be approximated by the expression

$$R = R_0 \left[C_4 \left(\frac{v}{v_0} - 1 \right)^2 + 1 \right], \quad (8)$$

where the constants R_0 and C_4 are function of the working conditions.

The equations (3)–(8) represent empirical laws obtained by the observations of the averaged values of the variables. Because of the absence of the instantaneous variations of the variables, we shall assume that these relations hold true for the instantaneous values, too. Transition to the dynamical description of the cutting process is made by changing the averaged values h, v, v_f into quantities function of time:

$$h(t) = h_i - y(t), \ v(t) = v_i - \dot{x}(t),$$

$$v_f(t) = \frac{v(t)}{R(t)} - \dot{y}(t), \qquad (9)$$

relations that will be replaced in the expressions of the cutting force components.

Let us remark that the tool's oscillations can lead to situation for which $y > h$, $\dot{x} > v_i$ or $v_f < 0$. For these reasons we shall complete the previous relations with the conditions

$$F_x = 0 \ \text{for} \ h < 0 \ \text{or} \ v < 0 \qquad (10)$$

and

$$K(-v_f) = K(v_f). \qquad (11)$$

These conditions can be written with the aid of the unity step Heaviside function

$$\Theta(x) = \begin{cases} 0 \ \text{for} \ x < 0 \\ 1 \ \text{for} \ x \geq 0 \end{cases} \qquad (12)$$

and of sign function

$$\text{sgn}(x) = \begin{cases} -1 \ \text{for} \ x < 0 \\ 0 \ \text{for} \ x = 0 \\ 1 \ \text{for} \ x > 0 \end{cases}. \qquad (13)$$

For the future analysis we shall introduce the normalized variables:

$$X = \frac{x}{h_0}, \ Y = \frac{y}{h_0}, \ T = t\frac{v_0}{h_0} = t\omega_0,$$

$$X' = \frac{dX}{dT} = \frac{\dot{x}}{v_0}, \ Y' = \frac{dY}{dT} = \frac{\dot{y}}{v_0}, \ H_i = \frac{h_i}{h_0},$$

$$H = H_i - Y, \quad V_i = \frac{v_i}{v_0}, \quad V = V_i - X'. \quad (14)$$

The dynamics of the cutting process is represented by two non-linear equations, which, in normalized form, read

$$X'' + C_X X' + K_X X = F,$$

$$Y'' + C_Y Y' + K_Y Y = KF, \qquad (15)$$

where:

$$F = F_0 H \left[C_1 (V-1)^2 + 1 \right], \qquad (16)$$

$$K = K_0 \left[C_2 (V_f - 1)^2 + 1 \right] \times$$
$$\left[C_3 (H-1)^2 + 1 \right] \Theta(F) \text{sgn}(V_f), \qquad (17)$$

$$R = R_0 \left[C_4 (V-1)^2 + 1 \right], \qquad (18)$$

$$V_f = V - RY', \qquad (19)$$

$$K_X = \frac{k_x}{m\omega_0^2} = \left(\frac{\omega_x}{\omega_0} \right)^2, \qquad (20)$$

$$K_Y = \frac{k_y}{m\omega_0^2} = \left(\frac{\omega_y}{\omega_0} \right)^2, \qquad (21)$$

$$C_X = \frac{c_x}{m\omega_0}, \qquad (22)$$

$$C_Y = \frac{c_y}{m\omega_0}, \qquad (23)$$

$$F_0 = \frac{F_{x_0}}{h_0 m\omega_0^2}. \qquad (24)$$

The instability of the cutting process is specially caused by the dependence of the cutting force on the speed (Fig. 3).
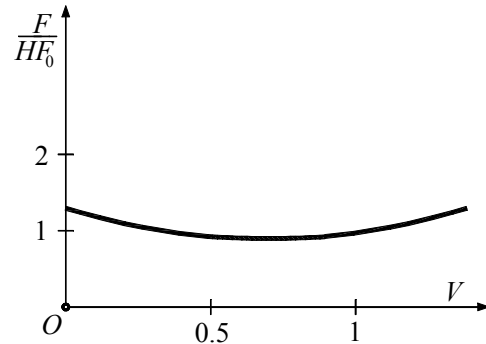

Fig. 3. The dependence of the cutting force on speed.

The dependence of the friction coefficient on the shear speed is qualitative similarly. As a consequence of the negative slope of the expressions which define F and K in function of speed, the non-linear oscillators can introduce a stick-slip phenomenon in the cutting process.

Let us remark that the oscillations exist even for zero initial conditions:

$$X(0) = Y(0) = X'(0) = Y'(0) = 0. \qquad (25)$$

3 The Working Parameters

For the numerical analysis we must specify the parameters of the working process. The following set of parameters corresponds to a large class of steels:

$C_1 = 0.3$, $C_2 = 0.7$, $C_3 = 1.5$, $C_4 = 1.2$,

$R_0 = 2.2$, $h_0 = 0.25 \, \text{mm}$, $v_0 = 6.6 \, \text{m/s}$,

$K_0 = 0.36$, $\omega_0 = 2.64 \times 10^4 \, \text{rad/s}$. (26)

Further on, these parameters will be kept constant.

The rest of the parameters depend on the working conditions and the machine-tool's properties.

The constants K_X and K_Y are determined by the resonance frequencies of the machine-tool at rest onto the two directions. Such a frequency is between 1 and $10 \, \text{kHz}$. It is normal to select as typical value for K_X the value

$$K_X = 1, \tag{27}$$

corresponding to

$$\omega_x = \omega_0. \tag{28}$$

The value K_Y is normally a few times smaller because of the lesser rigidity of the machine tool onto the y direction. We selected the value

$$K_Y = 0.25 \tag{29}$$

that corresponds to a twice lesser resonance frequency onto the y direction than onto the x direction.

Usually the viscous friction coefficient has very small values onto the two directions and for this reason we shall consider

$$C_X = C_Y = 0. \tag{30}$$

The last, but the most important parameter is F_0. Depending on this parameter we determine the amplitude of the cutting force. It is proportional (in an approximate way) to the width of the chip. In addition, the structure of the equations (15) shows that the increasing of F_0 leads to the increasing of the vibrations' amplitudes in the system. A typical value of the parameter F_0 at which we expect non-linear effects in the system is given by

$$F_0 = 0.5. \tag{31}$$

4 Numerical Analysis

Based on the experimental results, we shall consider two cases for the numerical simulation. The first case is characterized by

$$H_i = 0.4, \ V_i = 1.31, \tag{32}$$

and the second case is characterized by

$$H_i = 1.2, \qquad V_i = 1.38. \tag{33}$$

Denoting

$$Z_1 = X, \ Z_2 = Y, \ Z_3 = X', \ Z_4 = Y', \tag{34}$$

one obtains a system of four first order non-linear differential equations.

For this system's integration we select the following working parameters:

$$\Delta T = 0.025, \tag{35}$$

$$N_{iter} = 1.6 \times 10^4. \tag{36}$$

The initial conditions are

$$Z_1^0 = 0.6, \ Z_2^0 = 0.3, \ Z_3^0 = 0, \ Z_4^0 = 0. \tag{37}$$

In Fig. 4, a) we captured the time history for the variable Z_1 in the first case, and in Fig. 4, b) we captured the time history for the variable Z_4 in the second case. The time history for the rest of the variables is similar to these two in both cases. These diagrams suggest that after a transitory period (specific to each variable) the motion stabilizes, that

is we obtain a stable cutting regime. This means that, from the Grabec model's point of view, the parameters were chosen inside the stability lobes. Unfortunately, this behavior is not the real behavior observed in the experiments.
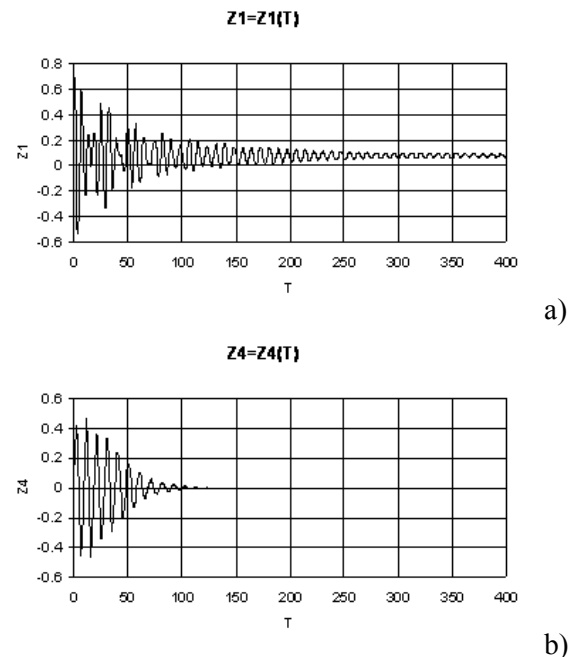

Fig. 4. Time history of a significant variable: a) the variation $Z_1 = Z_1(T)$ for $T \in [0,400]$ in the first case; b) the variation $Z_4 = Z_4(T)$ for $T \in [0,400]$ in the second case.

During the experiments we observed that the motion is not stable and, in addition, it presents a complete fortuitous behavior that makes us to believe that we deal with a chaotic dynamics.

For this reason we create a new model to correspond to the reality.

5 The New Model

We consider an orthogonal grinding machine where the cutting edge is parallel to the work-piece surface and normal to the cutting direction (see Fig. 5). We assume that the depth of cut, denoted by w, is much smaller than the cutting width. The tool and the work-piece have rotational motions with angular speed ω_t and ω_w, respectively. In what follows, the indexes t and w refer to the grinding wheel and to the work-piece respectively. In Fig. 5, a) w_s denotes the pre-set value for the depth of cut. The work-piece, considered homogeneous and infinitely long in the z-direction, moves in this direction with velocity v_{fs}, v_{fs} and v_w denote the pre-set values for the feeding speed and the tangential velocity of

the work-piece, respectively. Due to the cutting force the tool is deformed. Its visco-elastic and inertial properties are described by a two degrees of freedom oscillator, which is presented in Fig. 5, b). We assume that the work-piece also vibrates, but only in the y-axis direction. Its visco-elastic and inertial properties are therefore described by a one-degree of freedom oscillator, shown in Fig. 5, c).

The state variables of the process are the displacement of the cutting edge in the (x, y) directions and of the work-piece in the y direction (x_t, y_t, y_w). The dynamics of these state variables is given by the following differential equations:

$$m_t \ddot{x}_t + c_{tx} \dot{x}_t + k_{tx} x_t = F_x,$$
$$m_t \ddot{y}_t + c_{ty} \dot{y}_t + k_{ty} y_t = F_y,$$
$$m_w \ddot{y}_w + c_w \dot{y}_w + k_w y_w = -F_y. \tag{38}$$

The friction velocity in the direction of the y-axis is given by $v_f = \dfrac{v}{R}$, where R is a factor due to plastic shear deformation, which value is

$$R = R_0 \left[C_4 \left(\frac{v}{v_0} - 1 \right)^2 + 1 \right]. \tag{39}$$
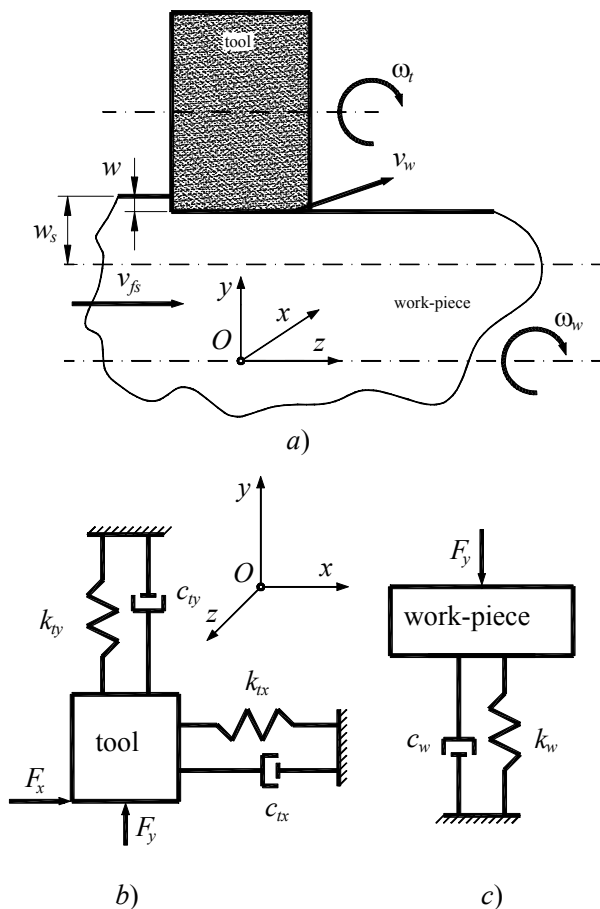

a)

b)   *c)*

Fig. 5. A model for orthogonal grinding.

In addition, the following instantaneous relations are satisfied:

$$w(t) = w_s - y_t(t) + y_w(t), \tag{40}$$
$$v(t) = v_w - \dot{x}_t(t) \tag{41}$$
$$v_f(t) = \frac{v(t)}{R(t)} - \dot{y}_t(t) + \dot{y}_w(t). \tag{42}$$

In Equations (38) we assume that the inertial mass of the tool is the same for both directions x and y. The dependence between the components F_x and F_y of the cutting force is expressed by

$$F_y = K_F \cdot F_x, \tag{43}$$

where K_F is a friction coefficient. According to the experimental data, the component Z_6 of the cutting force is of the form

$$F_x \propto w^{0.6}. \tag{44}$$

Using that dependence on the depth of cut, and otherwise following Grabec for the dependence on the velocity v, the expressions of the cutting force F_x, and friction coefficient K_F are then taken as:

$$F_x = F_{x_0} \left(\frac{w}{w_0} \right)^{0.6} \left[C_1 \left(\frac{v}{v_0} - 1 \right)^2 + 1 \right] \Theta(w)\Theta(v), \tag{45}$$

$$K_F = K_{F_0} \left[C_2 \left(\frac{v_w}{v_0} - 1 \right)^2 + 1 \right] \times$$
$$\times \left[C_3 \left(\frac{w}{w_0} - 1 \right)^2 + 1 \right] \Theta(F_x) \operatorname{sgn}(v_f), \tag{46}$$

where Θ is the Heaviside function and sgn is the sign function. The parameters F_{x_0}, w_0, v_0, K_{F_0}, C_1, C_2, C_3, C_4, R_0 denote specific cutting conditions. Due to the exponent 0.6 in relation (44), the present model exhibits a higher non-linearity.

6 Dimensionless System

We shall introduce the non-dimensional time as

$$T = t \frac{v_0}{w_0} = t\omega_0. \tag{47}$$

Using the dimensionless variables:

$$X_t = \frac{x_t}{w_0}, \tag{48}$$

$$Y_t = \frac{y_t}{w_0}, \tag{49}$$

$$Y_w = \frac{y_w}{w_0}, \tag{50}$$

$$V_w = \frac{v_w}{v_0}, \tag{51}$$

$$V = V_w - X_t', \tag{52}$$

$$W_S = \frac{w_s}{w_0} \tag{53}$$

$$W = W_s - Y_t + Y_w \tag{54}$$

and the notations:

$$C_{tx} = \frac{c_{tx} w_0}{m_t v_0} = \frac{c_{tx}}{m_t \omega_0}, \tag{55}$$

$$K_{tx} = \frac{k_{tx} w_0^2}{m_t v_0^2} = \frac{k_{tx}}{m_t \omega_0^2}, \tag{56}$$

and similar,

$$F_0 = \frac{F_{x_0}}{m_t \omega_0^2 w_0}, \tag{57}$$

$$F_1 = \frac{F_{x0}}{m_w \omega_0^2 w_0^{0.6}} = F_0 \frac{m_t}{m_w} = \lambda F_0, \tag{58}$$

$$F = F_0 W^{0.6} \left[C_1 (V - 1)^2 + 1 \right] \Theta(W) \Theta(V), \tag{59}$$

$$F_w = F_1 W^{0.6} \left[C_1 (V - 1)^2 + 1 \right] \Theta(W) \Theta(V), \tag{60}$$

$$R = R_0 \left[C_4 (V - 1)^2 + 1 \right], \tag{61}$$

$$K_F = K_{F_0} \left[C_2 (V_f - 1)^2 + 1 \right] \tag{62}$$

$$\left[C_3 (W - 1)^2 + 1 \right] \mathrm{sgn}(V_f) \Theta(F),$$

$$V_f = V - RY_t' + RY_w', \tag{63}$$

$$X_t = Z_1, \; X_t' = Z_2, \; Y_t = Z_3, \; Y_t' = Z_4,$$

$$Y_w = Z_5, \; Y_w' = Z_6, \tag{64}$$

we obtain from the previous equations the non-dimensional system:

$$\frac{dZ_1}{dT} = Z_2, \; \frac{dZ_3}{dT} = Z_4, \; \frac{dZ_5}{dT} = Z_6 \tag{65.1}$$

$$\frac{dZ_2}{dT} = -C_{tx} Z_2 - K_{tx} Z_1 +$$

$$+ F_0 (W_s - Z_3 + Z_5)^{0.6} \times \tag{65.2}$$

$$\times \left[C_1 (V_w - Z_2 - 1)^2 + 1 \right] \Theta(W) \Theta(V),$$

$$\frac{dZ_4}{dT} = -C_{ty} Z_4 - K_{ty} Z_3 +$$

$$+ K_{F_0} F_0 (W_s - Z_3 + Z_5)^{0.6} \times$$

$$\times \left[C_1 (V_w - Z_2 - 1)^2 + 1 \right] \times$$

$$\times \left\{ C_2 \left\{ V_w - Z_2 + R_0 \left[C_4 (V_w - Z_2 - 1)^2 + 1 \right] \times \right. \right. \tag{65.3}$$

$$\times (-Z_4 + Z_6) - 1 \right\}^2 + 1 \right\} \times$$

$$\times \left[C_3 (W_s - Z_3 + Z_5 - 1)^2 + 1 \right] \times$$

$$\times \Theta(W) \Theta(V) \Theta(F) \mathrm{sgn}(V_f),$$

$$\frac{dZ_6}{dT} = -C_w Z_6 - K_w Z_5 -$$

$$\lambda K_{F_0} F_0 (W_s - Z_3 + Z_5)^{0.6} \times$$

$$\times \left[C_1 (V_w - Z_2 - 1)^2 + 1 \right] \times$$

$$\times \left\{ C_2 \left\{ V_w - Z_2 + R_0 \left[C_4 (V_w - Z_2 - 1)^2 + 1 \right] \times \right. \right. \tag{65.4}$$

$$\times (-Z_4 + Z_6) - 1 \right\}^2 + 1 \right\} \times$$

$$\times \left[C_3 (W_s - Z_3 + Z_5 - 1)^2 + 1 \right] \times$$

$$\times \Theta(W) \Theta(V) \Theta(F) \mathrm{sgn}(V_f).$$

7 Number of Critical Points

In this paragraph we consider the Heaviside and sign functions to be $\Theta = 1$ and $\mathrm{sgn} = 1$. The critical points of the system (65) are obtained by equating the right hand side terms of the system to zero. The first, second and third equation provide immediately the values:

$$Z_2 = 0, \; Z_4 = 0, \; Z_6 = 0, \tag{66}$$

which, replaced in the rest of the equations, lead to:

$$K_{tx} Z_1 + F_0 (W_s - Z_3 + Z_5)^{0.6} \times$$
$$\times \left[C_1 (V_w - 1)^2 + 1 \right] = 0, \tag{67.1}$$

$$- K_{ty} Z_3 + K_{F_0} F_0 (W_s - Z_3 + Z_5)^{0.6} \times$$
$$\times \left[C_1 (V_w - 1)^2 + 1 \right] \times \left[C_2 (V_w - 1)^2 + 1 \right] \times \tag{67.2}$$
$$\times \left[C_3 (W_s - Z_3 + Z_5 - 1)^2 + 1 \right] = 0,$$

$$- K_w Z_5 - \lambda K_{F_0} F_0 (W_s - Z_3 + Z_5)^{0.6} \times$$
$$\times \left[C_1 (V_w - 1)^2 + 1 \right] \times \left[C_2 (V_w - 1)^2 + 1 \right] \times \tag{67.3}$$
$$\times \left[C_3 (W_s - Z_3 + Z_5 - 1)^2 + 1 \right] = 0.$$

In these conditions, when $\Theta = 1$ and $\mathrm{sgn} = 1$, the inequation $Z_3 - Z_5 < W_s$ is always satisfied.

From the last two relations of the system (67) we now obtain

$$Z_5 = -\lambda \frac{K_{ty}}{K_w} Z_3 = \psi Z_3, \tag{68}$$

with $\psi < 0$.

The second relation of the system (67) can thus be written

$$K_{ty} Z_3 = K_{F_0} F_0 (W_s - Z_3 + \psi Z_3)^{0.6} \times$$
$$\times \left[C_1 (V_w - 1)^2 + 1 \right] \times \left[C_2 (V_w - 1)^2 + 1 \right] \times \tag{69}$$
$$\times \left[C_3 (W_s - Z_3 + \psi Z_3 - 1)^2 + 1 \right].$$

In the working interval $\left(0, \dfrac{W_s}{1 - \psi} \right)$, the left hand side term is a strictly increasing linear function,

while the right hand side term is a strictly decreasing function. In these conditions the equation (69), considered as an equation for the variable Z_3, has one and only one solution (Fig. 6). Therefore, there is also one solution for Z_1 and Z_5 and only one critical point.
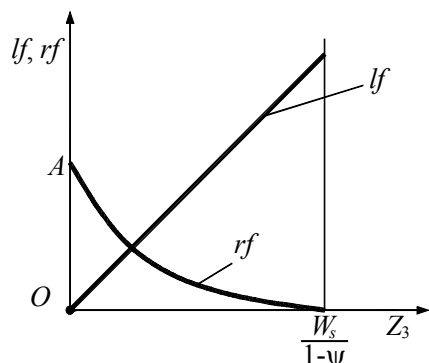

Fig. 6. The number of critical points.

8 Stability Analysis

Denoting by $f_i(Z_1, Z_2, Z_3, Z_4, Z_5, Z_6)$ the expressions of $\dfrac{\partial Z_i}{\partial T}$, $i = \overline{1, 6}$, and by j_{kl} the partial derivatives $\dfrac{\partial f_k}{\partial Z_l}$, $k = \overline{1, 6}$, $l = \overline{1, 6}$, we obtain the characteristic equation

$$\begin{vmatrix} -\lambda & 1 & 0 & 0 & 0 & 0 \\ j_{21} & j_{22} - \lambda & j_{23} & 0 & j_{25} & 0 \\ 0 & 0 & -\lambda & 1 & 0 & 0 \\ 0 & j_{42} & j_{43} & j_{44} - \lambda & j_{45} & j_{46} \\ 0 & 0 & 0 & 0 & -\lambda & 1 \\ 0 & j_{62} & j_{63} & j_{64} & j_{65} & j_{66} \end{vmatrix} = 0 . \quad (70)$$

Developing this determinant, one can observe that he or she obtains a polynomial equation of sixth degree. In addition, only 24 products have to be considered. Denoting by $(i_1, i_2, i_3, i_4, i_5, i_6)$ the product $a_{1i_1} a_{2i_2} a_{3i_3} a_{4i_4} a_{5i_5} a_{6i_6}$, where a_{kl}, $k = \overline{1, 6}$, $l = \overline{1, 6}$, are the components of the matrix given in the relation (33), the 24 products are: (1, 2, 3, 4, 5, 6), (1, 2, 3, 4, 6, 5), (1, 2, 3, 5, 6, 4), (1, 2, 3, 6, 5, 4), (1, 2, 4, 3, 5, 6), (1, 2, 4, 3, 6, 5), (1, 2, 4, 5, 6, 3), (1, 2, 4, 6, 5, 3), (1, 3, 4, 2, 5, 6), (1, 3, 4, 2, 6, 5), (1, 3, 4, 5, 6, 2), (1, 3, 4, 6, 5, 2), (1, 5, 3, 2, 6, 4), (1, 5, 3, 4, 6, 2), (1, 5, 4, 2, 6, 3), (1, 5, 4, 3, 6, 2), (2, 1, 3, 4, 5, 6), (2, 1, 3, 4, 6, 5), (2, 1, 3, 5, 6, 4), (2, 1, 3, 6, 5, 4), (2, 1, 4, 3, 5, 6), (2, 1, 4, 3, 6, 5), (2, ,1, 4, 5, 6, 3), (2, 1, 4, 6, 5, 3).

Following references, the working parameters are as follows:

$$C_{tx} = 0 , \quad C_{ty} = 0 , \quad C_w = 0 , \quad (71)$$

$$K_{tx} = 1 , \quad K_{ty} = 0.25 , \quad K_w = 0.9 , \quad (72)$$

$$\lambda = 1 , \quad F_0 = 0.5 , \quad (73)$$

$$C_1 = 0.3 , \quad C_2 = 0.7 , \quad C_3 = 1.5 , \quad C_4 = 1.2 , \quad (74)$$

$$K_{F_0} = 0.36 , \quad (75)$$

$$R_0 = 2.2 . \quad (76)$$

We shall consider two cases based on typical experimental data.

The first case is characterised by

$$W_s = 0.4 , \quad V_w = 1.31 , \quad (77)$$

and the second one by

$$W_s = 1.2 , \quad V_w = 1.38 . \quad (78)$$

For these values, instabilities for the motions of the tool-work-piece system were observed.

For the first considered case one finds the following values for the critical point co-ordinates:

$$Z_1 = 0.07671 , \quad Z_3 = 0.28022 ,$$

$$Z_5 = -0.07784 ; \quad (79)$$

for the second case the critical point is given by:

$$Z_1 = 0.25619 , \quad Z_3 = 0.69989 ,$$

$$Z_5 = -0.19441 . \quad (80)$$

A standard linear stability analysis of this critical point leads to the characteristic equation

$$\lambda^6 + 0.58544\lambda^5 + 2.29853\lambda^4 + 0.84301\lambda^3 +$$
$$+ 1.55931\lambda^2 + 0.25414\lambda + 0.28187 = 0 \quad (81)$$

for the first case.

In the second case the characteristic equation is

$$\lambda^6 + 0.49244\lambda^5 + 2.43827\lambda^4 + 0.70483\lambda^3 +$$
$$1.80460\lambda^2 + 0.20105\lambda + 0.36707 = 0 , \quad (82)$$

where λ is the complex rate of growth of the perturbation. It was checked that in both cases the six order determinant for the Routh-Hurwitz criterion has negative values.

Thus, the critical point is unstable in the linear approximation, and it is therefore unstable in the original system.

9 Numerical Analysis

Due to the complex form of the system (65) a numerical solution is looked for. The working parameters are described in the previous section. In addition, we consider

$$\Delta T = 0.025 , \quad (83)$$

$$N_{iter} = 1.6 \times 10^4 . \quad (84)$$

The initial conditions are:

$$Z_1 = 0.6 , \quad Z_2 = 0.3 , \quad Z_3 = 0 ,$$

$$Z_4 = 0 , \quad Z_5 = 0 , \quad Z_6 = 0 . \quad (85)$$

One can observe the existence of a transient regime in the studied cases (see Fig. 7, a)). A clear transition exists between this regime and the rest of the time series. The situation is quite different for different variables, i. e. the route to the second regime and its length differ from variable to variable. Beyond the transient regime, the time series presents irregularity and looks random. In our study we have a six-dimension phase space. We represent projections on two dimensions of this space (see Fig. 7, b)). A characteristic of chaotic motion is that its portrait in the phase space is defined by a non-closed curve which occupies a well-defined zone. This characteristic appears very clearly in the figures, which show both linear instability and global stability of the critical point.

The non-linearity of the cutting force is clearly seen in Fig. 8. It has two reasons: the first one is its dependence on the depth of cut. The second is the use of the Heaviside function to represent the loss of contact between the tool and the work-piece. The reader can observe that there is no rule for the determination of the period when the tool is in contact with the work-piece and when it is not. This variation of the cutting force is at the origin of the waving form of the work-piece surface.

The reader is now asked to refer to Fig. 9, a) showing the entropy of the system. The entropy is a measure of the disorder degree in the system. It is clear from Fig. 9, a) that the entropy has large values, which is a property of a chaotic system, among others.

One can observe that the power spectra are continuous with broad-band basis and peaks (see Fig. 9, b)) due to the periodical components of the flow. This aspect of the power spectra is also compatible with chaos.

The Lyapunov exponents are calculated as functions of F_0 and W_s (see Fig. 10). It is known that a chaotic system is characterised by at least one positive Lyapunov exponent, the sum of Lyapunov exponents being negative. We have one well defined positive exponent (for the variable Z_1, see Fig. 10, a)) and the sum of Lyapunov exponents is negative. The convergence of all the above results is a clear indication that the dynamics is indeed chaotic.

Referring now to the Fig. 10, b) and c) one can see that if the Lyapunov exponent for the variable Z_1 (this variable is the displacement in the x-direction) increases, the Lyapunov exponent for the variable Z_2 (the velocity in the x-direction) decreases when the depth of cut W_s increases. This phenomenon is indicative of the transformation of

the energy input into potential energy (given by displacement) or in kinetic energy (given by velocity). For this reason we believe that the Lyapunov exponents can be considered a measure of the transformation of energy.
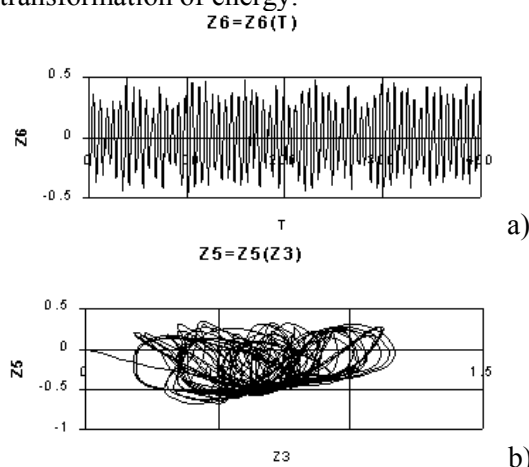
a)

b)

Fig. 7. a) Variation of Z_6 versus T for the second case. One can observe a period of transition for T between 0 and 25 time units; b) Variation of Z_5 versus Z_3 for the second case. Initial conditions are $Z_1 = 0.26$, $Z_2 = 0$, $Z_3 = 0.70$, $Z_4 = 0$, $Z_5 = -0.2$, $Z_6 = 0$. The critical point is at $Z_1 = 0.25619$, $Z_3 = 0.69989$, $Z_5 = -0.19441$. The reader can easy see the instability of the critical point, as well as its global stability.
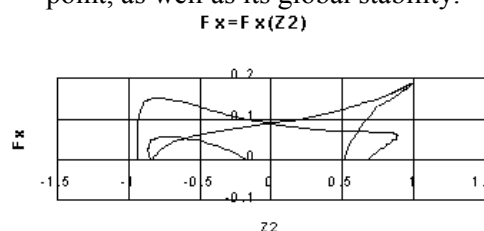
Fig. 8. Variation of the force F_x versus Z_2 in the first case. One can observe the cross points and zone where the force is null (i. e. the tool looses the contact with the work-piece). Time T was elected between 100 and 300 time units.

The Lyapunov dimension of the strange attractor is calculated by using the Kaplan-Yorke conjecture. For our model we found the dimension of the strange attractor to be between 5.3 and 5.9 (see Fig. 10, d)). This value proves that all six variables are needed to describe the chaotic dynamics of the system and that there is no reduction in the number of variables. In Grabec's model (which considered only four variables) the dimension of strange attractor was found between 2.4 and 2.7. In addition, the dimension of the strange attractor implies that previous models did not capture all the dynamics.
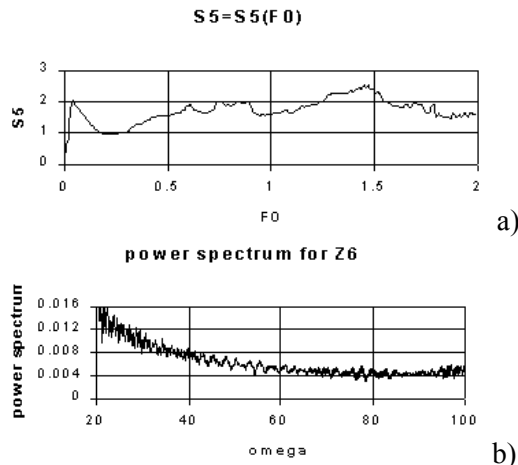
S 5 = S 5 (F 0)

a)

power spectrum for Z6

b)

Fig. 9. a) Variation of the entropy for the variable Z_5 versus F_0 in the second case; b) Power spectrum for the variable Z_6 in the second case.

Our model considers the interaction between the work-piece and the rest of the system, which is a new approach in comparison with the previous models. We also found different regimes for the transformation of energy (kinetic, elastic) inside the chaotic region.

All the results presented above lead to the conclusion that there exists a chaotic regime in the grinding processes.

10   CONCLUSIONS

The reader can easily observe that the Grabec model is a simplification that doesn't offer a correct representation of the cutting process. This inconvenient is a result of the fact that Grabec model considers only the vibrations of the tool, and the work-piece has no motion. To obtain a good model of the real cutting process we were constrained to create a new, more complex model. In our paper we presented a non-linear model with three degrees of freedom for the external cylindrical grinding. We considered the vibrations of the tool in two directions and the vibrations of the work-piece in one direction. The instability of the cutting process stems from three factors: the dependence of the cutting force on the feeding velocity and the depth of cut, and the dependence of the friction coefficient on the friction velocity. We obtained the expression of the characteristic equation in the most general cases and we showed that only 24 products (instead of 720 for a six order determinant) are necessary to calculate the coefficients of the characteristic equation. We proved the existence of one critical point and its linear instability for the considered values. We also proved unambiguously the existence

of chaos from the clear convergence of indications from various methods of different nature. Furthermore, different regimes for the transformation of the input energy were found in the chaotic region, either in elastic energy or in kinetic energy, depending on the depth of cut. The question arises of what is the number of relevant variables in order to describe the chaotic dynamics of the system when the model includes a high number of degrees of freedom, or in other words, if there is a significant reduction in the number of variables in such models. This will be the object of future work.
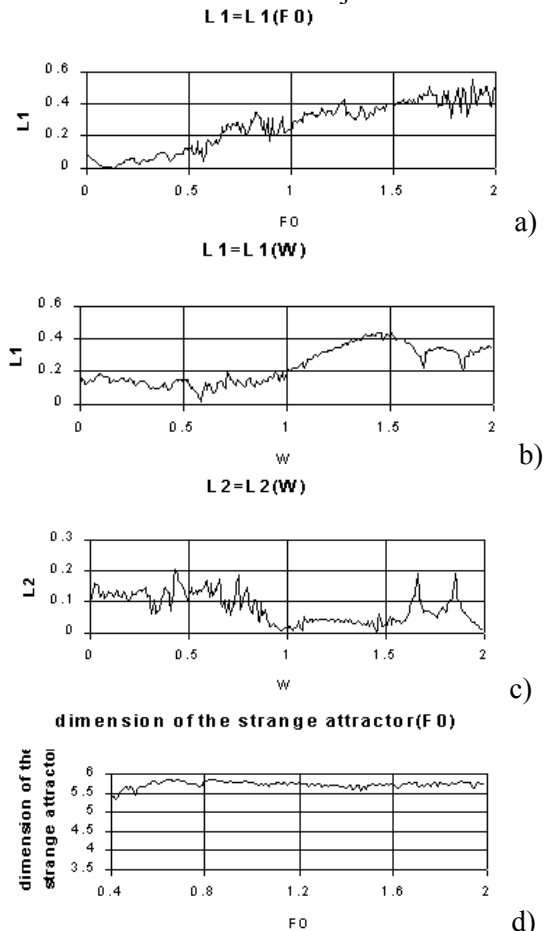
L 1 = L 1 (F 0)

a)

L 1 = L 1 (W)

b)

L 2 = L 2 (W)

c)

dimension of the strange attractor(F 0)

d)

Fig. 10. a) Lyapunov exponent for Z_1 versus F_0. In this case $W_s = 0.4$ and $V_w = 1.31$. The reader can observe that this Lyapunov exponent is positive; b) Lyapunov exponent for Z_1 versus W_s. In this case $F_0 = 0.5$ and $V_w = 1.38$. The reader can see that this Lyapunov exponent is positive; c) Lyapunov exponent for Z_2 versus W_s. In this case $F_0 = 0.5$ and $V_w = 1.38$. The reader can see that this Lyapunov exponent is positive; d) Dimension of the strange attractor versus F_0 in the first case. One can see that this dimension is between 5.3 and 5.9.

References:

[1] Merrit H. E., Theory of self-excited machine-tool chatter, Contribution of machine-tool chatter research-1, *Transactions of ASME, Journal of Engineering for Industry*, Vol 87, No. 4, 1965, pp. 447-454.

[2] Tobias S. A., *Machine-Tool Vibrations*, Blackall, London, 1965.

[3] Tlusty J., *Machine Dynamics* in R. I. King (Ed.) *Handbook of High Speed Machining Technology*, Chapman and Hall, New York, 1985.

[4] Abarbanel H. D. I., *Analysis of Observed Chaotic Data,* Springer-Verlag, New York, 1996.

[5] Grabec I., Chaos generated by the cutting process, *Physics Letters A*, Vol. **117**, No. 8, 1986, pp. 384-386.

[6] Grabec I., Chaotic dynamics of the cutting process *International Journal of Machine Tools & Manufacture*, Vol. 28, 1988, pp. 2179–2185.

[7] Potočnik P., Grabec. I., Non-linear model predictive control of a cutting process *Neurocomputing*, Vol. 43, 2002, pp. 107–126.

[8] Picoş C., Pruteanu O., Bohosievici C., Coman Gh., Braha V., Paraschiv D., Slătineanu L., Grămescu T., Marin A., Ionesii V., Toca A., *Proiectarea Tehnologiilor de Prelucrare Mecanică prin Aşchiere*, Universitas, Chişinău, 1992 (in Romanian).

[9] Gans R. F., When is cutting chaotic, *Journal of Sound and Vibration*, Vol. 188, No. 1, 1995, pp. 75-83.

[10] Kaplan J. L., Yorke J. A., in: H. O. Peitgen and H. O. Walther (Ed.), *Functional Differential Equations and Approximation of Fixed Points*, Springer, Berlin, 204, 1979.

[11] Lipinski P., Sinot O., Lefebvre A., Private communication.

[12] Stănescu, N.–D., Munteanu, L., Chiroiu, V., Pandrea, N., *Dynamical systems. Theory and applications, vol. 1*, The Publishing House of the Romanian Academy, Bucharest (Romania), 2007.

[13] Stănescu, N.–D., Munteanu, L., Chiroiu, V., Pandrea, N., *Dynamical systems. Theory and applications, vol. 2*, The Publishing House of the Romanian Academy, Bucharest (Romania), 2009 (in press).

[14] Pandrea, N., Stănescu, N.–D., *Mechanics*, Didactical and Pedagogical Publishing House, Bucharest (Romania), 2002.

[15] Stănescu, N.–D., *Numerical methods*, Didactical and Pedagogical Publishing House, Bucharest (Romania), 2007.